

## Saturation Effects in Paramagnetic Resonance\*†

A. H. ESCHENFELDER‡ AND R. T. WEIDNER

*Department of Physics, Rutgers University, New Brunswick, New Jersey*

(Received July 28, 1953)

Saturation effects have been observed in the paramagnetic resonance absorption of 3.2-cm microwaves by diluted samples of iron ammonium alum and chromium potassium alum at 2 to 4°K. For all samples the spin-lattice relaxation time  $T_1$  was found to vary inversely with the temperature, in agreement with theoretical expectation that the direct rather than the "Raman" process for the spin-lattice quantum transfer predominates at helium temperatures. Diluted samples of iron ammonium alum with iron to aluminum atom ratios of 1:18, 1:59, and 1:80 showed  $T_1$  to be essentially independent of dilution and yielded  $TT_1 = 5 \times 10^{-4}$  sec °K for the  $m = \frac{1}{2} \rightarrow -\frac{1}{2}$  transition. The low-field side peak in the iron alum spectrum for the (100) orientation, comprised of two unresolved transitions, yielded an effective value of  $TT_1 = 1.4 \times 10^{-3}$  sec °K. The  $m = \frac{1}{2} \rightarrow -\frac{1}{2}$  transition for diluted chromium alum with a chromium to aluminum atom ratio of 1:10 yielded  $TT_1 = 3 \times 10^{-3}$  sec °K in agreement with the calculated value. In all samples the spin-spin relaxation time was found to be temperature independent and of the order of  $10^{-9}$  sec. The results for  $T_1$  are at variance with those obtained with low-frequency paramagnetic relaxation experiments, which show a faster temperature dependence than  $T^{-1}$  and an increase in  $T_1$  with dilution.

### I. INTRODUCTION

THE temperature dependence of the spin-lattice relaxation time,  $T_1$ , in paramagnetic salts depends upon which of two relaxation processes dominates in the transfer of energy between the lattice vibrations and the spin system. In the direct, or first-order, process a single quantum of lattice vibration is transferred between the spin and lattice systems; in the second-order, Raman-like process the lattice absorbs a quantum of one frequency and scatters a quantum of another frequency. It is theoretically expected that the first-order process will control the relaxation at low temperatures, leading to a  $T_1$  temperature dependence of  $T^{-1}$  for chromium and iron alums in the liquid helium region.<sup>1</sup> For higher temperatures the Raman process should be effective, causing the relaxation time in these salts to exhibit a  $T^{-7}$  behavior. Experiments using the technique of paramagnetic relaxation at audio-frequencies with chromium and iron alum indicate,<sup>2-5</sup> however, a  $T_1$  temperature dependence that is appreciably faster than  $T^{-1}$  in the liquid helium region. These experiments suggest then that the second-order process is at least partially effective in this temperature range.

The purpose of the experiment reported here was to measure the temperature dependence of  $T_1$  at helium temperatures of chromium potassium sulfate and iron ammonium sulfate by an independent method, that of the saturation effect in paramagnetic resonance ab-

sorption at 3.2-cm wavelength. The saturation method, when used with salts for which the lines of the resonance spectrum are well resolved, permits the detailed study of transitions between separate pairs of energy levels and the evaluation of  $T_1$  for a particular transition. On the other hand, the low-frequency relaxation measurements, in which  $T_1$  is evaluated by examining the behavior of the bulk susceptibility of the sample, yield a value of  $T_1$  which is an average for all possible transitions between magnetic levels.

### II. THEORY

Spin-lattice relaxation effects are evidenced in paramagnetic resonance absorption when the power level is sufficiently high to disturb the Boltzmann distribution of the spins. Then the power absorbed in magnetic resonance is not proportional to the incident power at high power levels, but rather shows saturation.

If the separations of the magnetic energy levels of the paramagnetic salt is small compared with  $kT$ , the absorbed power at a resonance peak,  $P_a$ , is given by

$$P_a = \frac{N(h\nu)^2 W_i}{(2S+1)kT(1+W_i/W_s)}, \quad (1)$$

where  $N$  is the number of spins in the paramagnetic salt,  $\nu$  is the microwave frequency,  $S$  is the total spin quantum number,  $W_i$  is the transition probability for induced transitions, and  $W_s$  is the spontaneous transition probability characterizing the spin-lattice relaxation. The spin-lattice relaxation time  $T_1$  is defined as  $1/2W_s$ .

If one assumes that only magnetic dipole transitions occur between unequally spaced Zeeman levels,  $M \rightarrow M-1$ ,

$$W_i = \frac{1}{4}g(\nu)_m \gamma^2 H_1^2 (S+M)(S-M+1), \quad (2)$$

where  $\gamma$  is the gyromagnetic ratio ( $2\pi\nu/H_0$ ),  $H_1$  is the amplitude of the circulating magnetic field effective in

\* This work was supported by the U. S. Office of Naval Research, the Rutgers University Research Council, and the Radio Corporation of America.

† Based on the Ph.D. thesis submitted by A.H.E. to the Graduate School of Rutgers University.

‡ Now at International Business Machines Corporation, Poughkeepsie, New York.

<sup>1</sup> J. H. Van Vleck, *Phys. Rev.* **57**, 426 (1940).

<sup>2</sup> Kramers, Bijl, and Gorter, *Physica* **16**, 65 (1950).

<sup>3</sup> D. Bijl, Thesis, Leiden, 1950 (unpublished).

<sup>4</sup> R. J. Benzie and A. H. Cooke, *Proc. Phys. Soc. (London)* **A63**, 201 (1950).

<sup>5</sup> F. W. de Vrijer and C. J. Gorter, *Physica* **18**, 549 (1952).

resonance absorption, and  $g(\nu)_m$  is the maximum value of the shape function of the absorption line. The spin-spin relaxation time  $T_2$  is  $\frac{1}{2}g(\nu)_m$  when the line is characterized by a Lorentz shape. Inasmuch as  $W_i$  is proportional to the microwave energy, Eq. (1) shows that saturation is significant at power levels for which  $W_i$  is comparable to  $W_s$ .

The common procedure for determining  $T_1$  has been that of examining the saturation term,  $W_i/W_s = \frac{1}{2}\gamma^2 H_1^2 \times g(\nu)_m T_1 (S+M)(S-M+1)$ . When the saturation term = 1, as indicated by the halving of the absorbed power per incident power or by the broadening of the line,  $T_1$  can be evaluated providing  $H_1^2$  and  $g(\nu)$ , or  $T_2$ , are known. In the procedure described below and used in our measurements it is possible to determine  $T_1$  without recourse to a separate evaluation of  $H_1^2$  and  $g(\nu)$ .

The paramagnetic salts were placed in a resonant cavity in order to increase the microwave magnetic energy density at the sample. The power absorbed in the salt,  $P_a$ , was measured as a function of the incident power by measuring the reflection coefficient looking into the cavity.

The cavity system can be considered equivalent to a series *RLC* circuit which is coupled to a line of characteristic impedance,  $Z_0$ , containing a matched generator of voltage  $E$ . When the cavity is tuned to resonance at the peak of an absorption line, the reactive components vanish and the magnetic absorption appears as an additional equivalent resistance  $\omega L/Q_M$ , where  $Q_M$  is the absorption  $Q$  of the paramagnetic salt. The loaded  $Q$  of the cavity in the absence of magnetic absorption,  $Q_L$ , is  $\omega L/(R+Z_0)$ . Therefore, the total impedance looking into the cavity,  $Z$ , is given by

$$Z = R + (R+Z_0)Q_L/Q_M. \quad (3)$$

The power  $P_c$  absorbed in the loaded cavity system (including the generator impedance  $Z_0$ ) without magnetic absorption is then

$$P_c = E^2/(R+Z_0) = (4Z_0 P_i)/(R+Z_0), \quad (4)$$

where  $P_i$  is the incident microwave power.

The ratio of the energies stored in the cavity with and without magnetic absorption is  $(R+Z_0)^2/(Z+Z_0)^2$ , and from the definition of the  $Q$ 's,

$$\frac{Q_M}{Q_L} = \left( \frac{R+Z_0}{Z+Z_0} \right)^2 \frac{P_c}{P_a}. \quad (5)$$

Using Eq. (4),

$$Q_M/Q_L = [4Z_0(R+Z_0)P_i]/[(Z+Z_0)^2 P_a]. \quad (6)$$

The reflection coefficient  $\Gamma = (Z-Z_0)/(Z+Z_0)$  refers to the cavity at resonance and with the dc magnetic field,  $H_0$ , adjusted for a magnetic resonance peak. At appreciably higher dc fields, the magnetic absorption vanishes,  $Z=R$ , and  $\Gamma=\Gamma_0$ .

Therefore, Eq. (6) may be written

$$Q_M/Q_L = [2(1-\Gamma)^2 P_i]/[(1-\Gamma_0)P_a]. \quad (7)$$

Introducing Eqs. (1) and (2), Eq. (7) may be written

$$\frac{Q_M}{Q_L} = A \left( \frac{2T}{\gamma^2 H_1^2 g(\nu)_m (S+M)(S-M+1)} + TT_1 \right) \times P_i (1-\Gamma)^2, \quad (8)$$

where  $A = [4(2S+1)k]/[N(h\nu)^2(1-\Gamma_0)]$ .

But  $P_i(1-\Gamma)^2$  is a measure of the power that reaches the sample in the cavity without reflection at the cavity coupling hole, and is therefore proportional to  $H_1^2$ . Equation (8) can then be written

$$\frac{Q_M}{Q_L} = B \frac{T}{g(\nu)_m} + ATT_1 P_i (1-\Gamma)^2, \quad (9)$$

where  $B$  is a constant. A plot of  $Q_M/Q_L$  against  $P_i(1-\Gamma)^2$  yields a straight line whose slope is proportional to  $TT_1$  and whose intercept is proportional to  $T/g(\nu)_m$ . The  $Q$  ratio is evaluated by using

$$Q_M/Q_L = (1-\Gamma)/(\Gamma-\Gamma_0), \quad (10)$$

which follows from Eq. (3) and the definitions of  $\Gamma$  and  $\Gamma_0$ .

It is seen then that  $T_1$  can be determined without requiring the evaluation of  $H_1^2$  and  $g(\nu)_m$ . An order-of-magnitude value of  $g(\nu)_m$  can be arrived at by using the definition of  $Q_L$ ,

$$Q_L = \frac{\nu H_1^2 V_c}{2P_c} = \frac{\nu H_1^2 V_c}{4(1-\Gamma_0)P_i}, \quad (11)$$

where  $V_c$  is the cavity volume and a uniform energy density throughout the cavity volume is assumed. This relation determines  $H_1^2$  and, hence,  $B$  in Eq. (9).

### III. EXPERIMENTAL ARRANGEMENT

In Fig. 1 is shown a cross section of the resonant cavity coupled to the waveguide. The cavity was of the cylindrical re-entrant type, coupled to the waveguide by a hole in the broad face of the waveguide. The waveguide was short-circuited one-quarter waveguide wavelength from the coupling hole. The samples, in the shapes of toroids of rectangular cross section,

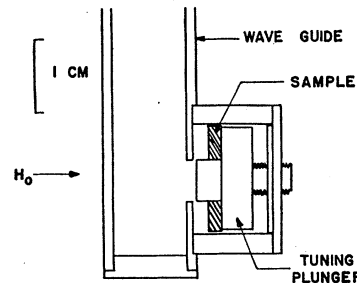


FIG. 1. The resonant cavity and sample.

were placed in the coaxial region of the cavity as shown. In this position the samples occupied a maximum part of the magnetic region of the cavity. The cavity was oriented with the dc field lines parallel to the cavity axis, thus assuring orthogonality of the dc and microwave magnetic fields.

For the re-entrant type resonant cavity the microwave magnetic field is not constant over the sample volume, and therefore  $H_1$  must be averaged over the sample. The absorbed power is given by Eq. (1) when  $H_1^2$  is constant over the sample volume and can be written in the form

$$P_a = \frac{KNW_i}{1 + (W_i/W_s)}, \quad (12)$$

where  $K$  is a constant. In the coaxial region of the re-entrant cavity  $H_1$  varies inversely with the radial distance  $r$ . Inasmuch as  $W_i$  is proportional to  $H_1^2$ , we may write  $W_i = c/r^2$ . But  $dN/N = 2rdr/(r_2^2 - r_1^2)$  is the fraction of spins between  $r$  and  $r + dr$ , and Eq. (12) becomes

$$P_a = \frac{2NKc}{r_2^2 - r_1^2} \int_{r_1}^{r_2} \frac{dr}{r(1 + c/W_s r^2)}, \quad (13)$$

where  $r_1$  and  $r_2$  are the inner and outer radii in the coaxial region respectively. For the cavity used,  $r_2/r_1 = 2.50$ .

Expanding the logarithm which results from the integral in Eq. (13),

$$P_a = \frac{NKW_i(r_2)}{1 + W_i(r_2)/W_s} \left[ 1 + \frac{0.42}{1 + W_i(r_2)/W_s} + \dots \right]. \quad (14)$$

With strong saturation  $W_i(r_2) \gg W_s$ , and Eq. (14) approaches Eq. (12), where  $W_i$ , however, refers to  $r_2$ . Thus Eq. (9) may be used without correction in the evaluation of  $T_1$  providing that severe saturation occurs. Tests with samples of varying thickness showed that axial variations in  $H_1^2$  may be neglected for samples that are sufficiently thin.

The metal cavity section was thermally insulated from the Dewar cap by a glass waveguide section thinly plated with silver. Liquid helium was allowed to fill the resonant cavity and lower waveguide section to assure good thermal contact with the sample. A 2K39 Sperry klystron with a power output of 1 watt was used as the 3.2-cm oscillator. The reflection coefficients  $\Gamma$  and  $\Gamma_0$  looking into the cavity arm were determined from the incident and reflected power as measured with a Magic- $T$  bridge. The incident power  $P_i$  was measured with a barretter bridge circuit.

The samples were prepared by recrystallization from saturated aqueous solutions. Single crystals of diluted iron ammonium alum with iron to aluminum atom ratios of 1:18, 1:59, and 1:80 as determined by chemical analysis were used; diluted samples of chromium potassium alum with a chromium to aluminum atom ratio of 1:10 were used.

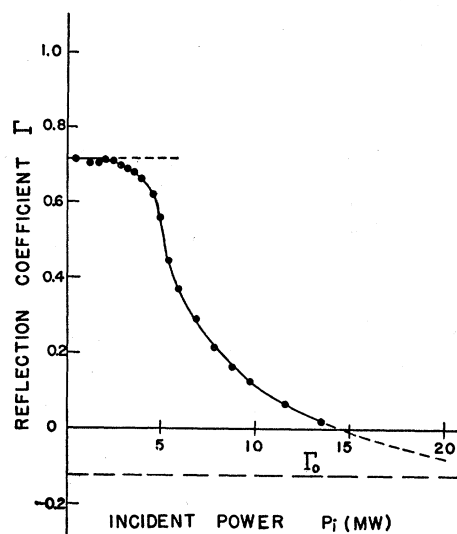


Fig. 2. Reflection coefficient looking into the sample-filled cavity as function of the incident microwave power

#### IV. RESULTS

The principal measurements on the iron alum samples were made with the dc field along the (100) axis. For this orientation the paramagnetic resonance spectrum is understood on the basis of the theory of Meijer.<sup>6</sup> The spectrum for diluted samples consists of a well-resolved, intense central peak ( $M = \frac{1}{2} \rightarrow -\frac{1}{2}$ ), a low-field side peak containing two unresolved lines ( $M = -3/2 \rightarrow -5/2$  and  $M = 3/2 \rightarrow 1/2$ ), and a high-field side peak containing two unresolved lines ( $M = 5/2 \rightarrow 3/2$  and  $M = -1/2 \rightarrow -3/2$ ).

Saturation measurements were made at the peaks of the resolved line,  $\frac{1}{2} \rightarrow -\frac{1}{2}$ , and the unresolved lines,  $-3/2 \rightarrow -5/2$  and  $3/2 \rightarrow 1/2$  for the (100) orientation; measurements with iron alum were also made using the  $\frac{1}{2} \rightarrow -\frac{1}{2}$  line in the (111) orientation, where this principal line is less well-separated from neighboring lines. The measurements with diluted potassium chrome alum were made using the  $\frac{1}{2} \rightarrow -\frac{1}{2}$  line in the (111) orientation, for which this transition is best resolved.

The results for a typical run are shown in Figs. 2 and 3. The sample in this case was 0.454 g of iron alum diluted 1:59, at 4.23°K. The measurements were made with the field adjusted to the central peak at about 3300 oersteds. Figure 2 shows the reflection coefficient plotted against the power incident on the cavity. At very low-power levels  $\Gamma$  is essentially constant; but as the power is increased and the saturation becomes appreciable,  $\Gamma$  approaches  $\Gamma_0$ , that is, the resistive losses overpower the magnetic losses. The sign of  $\Gamma$  is determined by observing whether magnetic absorption causes the power reflected from the cavity to increase or decrease, corresponding respectively to a positive or negative value of  $\Gamma$ . The  $\Gamma_0$  value was determined at a

<sup>6</sup> P. H. E. Meijer, *Physica* 17, 899 (1951).

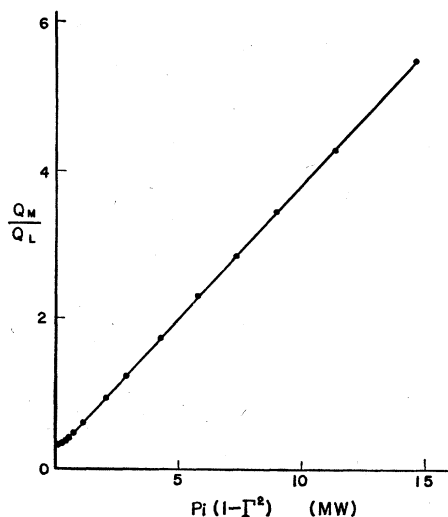


FIG. 3. Ratio of magnetic  $Q$  to loaded cavity  $Q$  as a function of the microwave power striking the sample.

dc field of about 6000 oersteds, far from the absorption lines.

In Fig. 3  $Q_M/Q_L$  is plotted against  $P_i(1-\Gamma)^2$  in accordance with Eqs. (9) and (10), using the data shown in Fig. 2. The points lie on a straight line as expected, except for points near the intercept, where the departure from linearity is to be attributed to the radial inhomogeneity of the microwave magnetic field in the cavity. The extreme plotted point in Fig. 3 corresponds to a saturation term ( $W_i/W_s$ ) of 22; thus the approximation used in Eq. (12), assuming severe saturation, is justified. Only those data which showed a linear  $Q_M/Q_L$  versus  $P_i(1-\Gamma)^2$  plot and which satisfied the severe saturation condition were considered acceptable; on this basis it was found that data for some samples and at some temperatures could not be used because unfavorable cavity coupling conditions precluded measurements at strong saturation conditions.

The loaded cavity  $Q$ ,  $Q_L$ , which was measured by observing  $\Gamma_0$  as a function of frequency and used in the approximate evaluation of  $g(\nu)_m$ , was found to be about 300; therefore, losses in the waveguide leading to the sample cavity could properly be neglected.

The results are shown in Fig. 4, where the logarithm of  $TT_1$  is plotted against  $T$ . The data are identified according to the crystal used (iron ammonium or chromium potassium alum), the magnetic quantum numbers of the transition, the dilution in terms of magnetic ions to aluminum atoms, and the orientation of the crystal in the dc magnetic field. The observation that  $TT_1$  is independent of temperature over the range 2 to 4°K for a given sample corresponds to an inverse-temperature dependence of the spin-lattice relaxation time.

The data shown for the  $\frac{1}{2} \rightarrow -\frac{1}{2}$  transition in iron alum, diluted 1:59 and in the (100) orientation, arise from two samples of differing thicknesses, correspond-

ing to masses of 0.171 and 0.458 gram. Inasmuch as no obvious difference in the  $TT_1$  values for the two thicknesses appears, it can be assumed that the samples were thin enough so that no correction need be applied for the variation in microwave field along the cavity axis.

The results for the  $\frac{1}{2} \rightarrow -\frac{1}{2}$  transition at 3300 oersteds in iron alum with samples of varying dilution show that  $TT_1$  is close to  $5 \times 10^{-4}$  sec °K for dilutions from 1:18 to 1:80, the extremes differing by a factor of only 1.3. The combined transitions,  $3/2 \rightarrow 1/2$  and  $-3/2 \rightarrow -5/2$  at 3000 oersteds for iron alum yield  $TT_1 = 1.4 \times 10^{-3}$  sec °K, which is higher than the value for the  $\frac{1}{2} \rightarrow -\frac{1}{2}$  line. The absolute value of  $T_1$  is rendered uncertain for these transitions inasmuch as the data apply to the resultant peak of the two transitions, which are not exactly superimposed; the sizable difference in  $T_1$  values for the central and side peaks suggests, however, that the spin-lattice relaxation time may differ from one transition to another, neglecting the field dependence of  $T_1$ . The central line at 3300 oersteds in the spectrum of diluted chromium potassium alum in the (111) orientation shows  $TT_1 = 3.2 \times 10^{-3}$  sec °K from 2° to 4°K. The spin-lattice relaxation time was thus found to be longer in the chromium alum than in the iron alum for corresponding temperatures.

It was observed that the absorption line widths increased with saturation; no attempt was made, however, to evaluate  $T_1$  from line widths because of the overlapping of adjacent lines and because of the un-

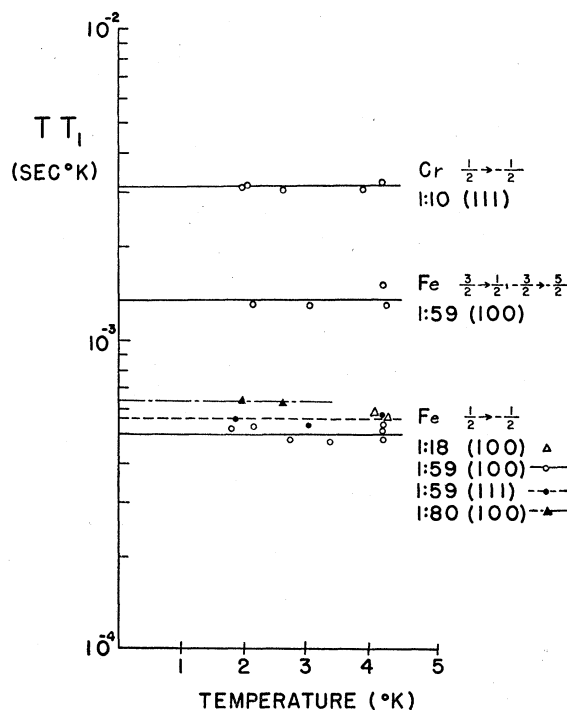


FIG. 4.  $TT_1$  as a function of temperature. The data are identified according to the salt, transition, dilution, and crystal orientation on the right.

certainties involved in taking account of exchange narrowing.

For any sample it was found that the intercepts in the  $Q_M/Q_L$  versus  $P_i(1-\Gamma)^2$  plot varied directly as the temperature; therefore,  $g(\nu)_m$  was found to be temperature independent, as is theoretically expected. All samples gave  $g(\nu)_m$  values of the order of  $4 \times 10^{-10}$  sec, corresponding to absorption line widths of about 300 oersteds, in agreement with the observed widths as to order of magnitude. The approximations involved in Eqs. (11) and (14) do not warrant more detailed evaluation of  $g(\nu)_m$  values.

## V. DISCUSSION

The inverse temperature dependence of  $T_1$  found for iron and chromium alums at helium temperature is in accord with theory but at variance with the paramagnetic relaxation measurements at audio-frequencies, which show a faster temperature dependence than  $T^{-1}$  for  $T_1$ .

Kramer, Bijl, and Gorter,<sup>2</sup> using three undiluted samples of iron alum at 3370 oersteds find  $T_1$  proportioned to  $T^{-n}$ , where  $n$  is between 4 and 5. The data are compatible with the assumption of a distribution of relaxation times rather than a single  $T_1$ . The values of  $T_1$  at 2° and 4°K, respectively, are  $1 \times 10^{-3}$  sec and  $7 \times 10^{-3}$  sec. The measurements of Benzie and Cooke<sup>4</sup> on undiluted iron alum at lower fields of from 205 to 968 oersteds show an exponent in the temperature dependence of  $n=2$  to 3; again a distribution of relaxation times was required to fit the data. Bijl<sup>3</sup> found  $T_1$  increasing rapidly as the magnetic dilution of the sample was increased using iron alum samples diluted 1 to 16 (iron to aluminum atoms) and 1 to 80; the more dilute sample indicated that  $T_1$  was greater than 0.02 sec at 4°K.

The results for chromium potassium alum are similar, showing a faster temperature dependence than  $T^{-1}$ , an increase in  $T_1$  with dilution, and a distribution of relaxation times. Vrijer and Gorter<sup>5</sup> give the results for measurements with an undiluted sample of chromium potassium alum over the temperature range 2° to 90°K at a field of 4000 oersted. These data are in harmony with the choice of a single exponent,  $n=2.6$ , over this range. The values of  $T_1$  at 2° and 4°K are  $7.8 \times 10^{-3}$  sec and  $1.3 \times 10^{-3}$  sec, respectively. The results of Kramers, Bijl, and Gorter<sup>2</sup> give a temperature exponent of 3 for 3370 oersteds with undilute chromium alum with  $T_1$  values of  $7.0 \times 10^{-3}$  sec and  $1.1 \times 10^{-3}$  sec for 2° and 4°K. Bijl<sup>7</sup> found that a dilute sample of chromium po-

tassium alum, with chromium to aluminum ratio of 1:13, followed a  $T^{-2}$  law with  $T_1$  values which were approximately 10 times larger than for the undilute samples.

The relaxation measurements are characterized by a lack of agreement among the several investigators as to the temperature exponent of  $T_1$ . The marked increase in  $T_1$  with dilution is surprising, as Eisenstein<sup>8</sup> remarks, because one expects  $T_1$  to depend only on the interaction of the spins with lattice via the spin orbit and orbit-lattice couplings. These anomalies have been attributed to chemical and physical impurities in the samples.

Van Vleck<sup>1</sup> has derived a relation giving the spin-lattice relaxation time for chromium potassium alum as a function of (among other things) the external field, the root-mean-square internal field, and the zero-field Stark splitting of the ground state. For fields of the order of 3300 oersteds, the calculated  $T_1$  values are relatively insensitive to a choice for the zero-field splitting, so that the two values found in paramagnetic resonance experiments with chromium potassium alum,<sup>9</sup> 0.15 cm<sup>-1</sup> and 0.27 cm<sup>-1</sup>, yield  $T_1$  values which differ by only ten percent. The calculated value  $TT_1$  is in agreement with measured value for chromium alum found here,  $TT_1=3.2 \times 10^{-3}$  sec °K, if 340 oersteds is chosen as the root-mean-square internal field. Van Vleck remarks that iron alum, for which no detailed calculations were made, as well as chrome alum, should follow a  $T^{-1}$  law at helium temperatures but that the  $T_1$  values for iron alum should be somewhat larger than those for chrome alum for any given temperature. The measurements here, however, show the reverse behavior,  $T_1$  for chrome alum exceeding that for iron alum.

The principal result of this experiment is the  $T^{-1}$  behavior of  $T_1$  for the diluted iron and chromium alums at liquid helium temperatures as determined by the saturation effect in paramagnetic resonance absorption at 3300 oersteds. This contrasts with the faster temperature dependence found with the paramagnetic relaxation method at audio-frequencies, but is in accord with theoretical predictions. For iron alum  $T_1$  is found to be essentially independent of dilution, whereas the relaxation measurements show a marked increase in  $T_1$  with dilution. These differences between the saturation and relaxation results are as yet unexplained and require further experiments for their resolution.

<sup>8</sup> J. Eisenstein, *Revs. Modern Phys.* **24**, 74 (1952).

<sup>9</sup> B. Bleaney, *Proc. Roy. Soc. (London)* **A204**, 203 (1950).

<sup>7</sup> D. Bijl, *Physica* **8**, 497 (1941).